Mon. Not. R. Astron. Soc. **371,** 1441–1447 (2006) doi:10.1111/j.1365-2966.2006.10768.x

No universality for the electron power-law index (p) in gamma-ray bursts and other relativistic sources

Rongfeng Shen,★ Pawan Kumar and Edward L. Robinson
Department of Astronomy, University of Texas at Austin, 1 University Station C1400, Austin, TX 78712, USA

Accepted 2006 July 4. Received 2006 May 27; in original form 2005 December 19

ABSTRACT

The gamma-ray burst (GRB) prompt emission is believed to be from highly relativistic electrons accelerated in relativistic shocks. From the GRB high-energy power-law spectral indices β observed by the Burst and Transient Source Experiment (BATSE) Large Area Detectors (LAD), we determine the spectral index, p, of the electrons' energy distribution. Both the theoretical calculations and numerical simulations of the particle acceleration in relativistic shocks show that p has a universal value $\approx$2.2–2.3. We show that the observed distribution of p during GRBs is not consistent with a δ-function distribution or a universal p value, with the width of the distribution $\geqslant$0.54. The distributions of p during X-ray afterglows are also investigated and found to be inconsistent with a δ-function distribution. The p distributions in blazars and pulsar wind nebulae are also broad, inconsistent with a δ-function distribution.

Key words: acceleration of particles – shock waves – methods: statistical – gamma-rays: bursts.

1 INTRODUCTION

Gamma-ray bursts (GRBs) are observed to have non-thermal spectra during the prompt emission phase (Band et al. 1993). It is widely believed that the synchrotron radiation and/or the inverse-Compton scattering are the likely emission mechanism(s) for the prompt hard X-ray and gamma-ray emission of GRBs. The electrons accounting for these emissions are thought to be accelerated in relativistic shocks in GRBs. According to the shock diffusive acceleration model, particles are accelerated when they repeatedly cross a shock front, and the competition between the particle's energy gain and escape probability per shock crossing cycle leads to a power-law spectrum for the particles

$$N(\gamma)\,\mathrm{d}\gamma \propto \gamma^{-p}\,\mathrm{d}\gamma, \tag{1}$$

where γ is the Lorentz factor of the particle (e.g. Blandford & Ostriker 1978). For non-relativistic shocks, the value of p depends on the compression ratio of the flow stream across the shock; while in relativistic or ultrarelativistic shocks, which are most likely the case in GRBs, analytical and numerical studies show that p has a 'universal' value, $\approx$2.2–2.3 (Bednarz & Ostrowski 1998; Kirk et al. 2000; Achterberg et al. 2001; Lemoine & Pelletier 2003).

The work reported in this paper is to investigate the 'universality' of the power-law index p for GRBs, which we calculate directly from the high-energy (0.1–2 MeV) photon spectrum of GRBs (Preece et al. 1998, 2000), assuming the spectrum is from synchrotron or synchrotron self-inverse-Compton (SSC) emission of the power-law distributed highly relativistic electrons, using the relations between p and the spectral index, β, of the high-energy power-law photon spectrum.

In Section 2, we describe the GRB spectral data set used and the process of determining the parent p distribution. In Section 3, we examine the contributions from the spectral fit procedure and the time-averaging effect to the dispersion of the parent distribution of p. The p distributions derived from *BeppoSAX* GRBs and from *HETE*-2 (*High Energy Transient Explorer*) GRBs, X-ray flashes (XRFs) and X-ray rich (XRR) GRBs are presented in Section 4. We determine the p distributions for X-ray afterglows in Section 5 and for blazars and pulsar wind nebulae (PWNe) in Section 6. The summary and discussions are given in Section 7.

2 THE DISTRIBUTION OF p IN GRBs

2.1 The GRB spectral sample

For our analysis, we use the Burst and Transient Source Experiment (BATSE) GRB spectral catalogue presented by Preece et al. (2000). In the catalogue, the time sequences of spectral fit parameters for 156 bright bursts are presented, using mostly the high-energy and time-resolution data from the Large Area Detectors (LAD), which cover an energy range of typically 28–1800 keV. All bursts have at least eight spectra in excess of 45σ above background. The spectral models used in the fit are (i) 'Band' function, (ii) Comptonized spectral model (a power law with an exponential cut-off), (iii) broken power-law model and (iv) smoothly broken power-law model. The 'Band' function, the one used most frequently, is an empirical

★E-mail: shenrf@astro.as.utexas.edu

function (Band et al. 1993)

$$N(E) = A \begin{cases} (E/100)^{\alpha} \exp[-E(2+\alpha)/E_{\rm peak}], & E < \frac{\alpha-\beta}{2+\alpha} E_{\rm peak} \\ \left[\frac{(\alpha-\beta)E_{\rm peak}}{100(2+\alpha)}\right]^{\alpha-\beta} \exp(\beta-\alpha)(E/100)^{\beta}, & E \geqslant \frac{\alpha-\beta}{2+\alpha} E_{\rm peak} \end{cases},$$

where $N(E)$ is the photon counts, A is the amplitude, α is the low-energy spectral index, β is the high-energy spectral index and $E_{\rm peak}$ is the peak energy in the νF_{ν} spectrum (when $\beta < -2$).

Since we are here caring about the high-energy power-law portion of the GRB spectra, and also because one possible source of systematic error in the spectral parameter determination arises in selecting different spectral models for different bursts (Preece et al. 2002), only the spectral parameters of those 'Band' function fitted spectra are selected for our analysis.

One of our major concerns is to select the sample of spectra for which β is reliably determined. The BATSE burst signal-to-noise ratio decreases at higher energies as a result of lower photon flux and the decreased detector efficiency. In particular, β may not be well determined if $E_{\rm peak}$ is close to the higher limit of the LAD energy range, $E_{\rm max}$ ($\approx$2 MeV) (Preece et al. 1998), thus we must choose those spectra with $E_{\rm peak}$ much lower than $E_{\rm max}$. Therefore, we select the spectra for which $100 < E_{\rm peak} < 200$ keV and the error in β is less than 0.1 $|\beta|$. This gives a total sample of 395 spectra for 78 bursts.

2.2 Distribution of *p* and its narrowing

For electron distribution given by a power law

$$N(\gamma_{\rm e}) \propto \gamma_{\rm e}^{-p}, \quad \text{for} \quad \gamma_{\rm e} > \gamma_{\rm min}, \tag{2}$$

the emergent high-energy synchrotron spectrum is asymptotically a power-law function $F_{\nu} \propto \nu^{-(p-1)/2}$ for $\nu_m < \nu < \nu_{\rm c}$ ('slow cooling' regime) and $\propto \nu^{-p/2}$ for $\nu > \nu_{\rm c}$ ('fast cooling' regime), where $\nu_m = \nu_{\rm syn}(\gamma_{\rm min})$ is the synchrotron injection frequency, and $\nu_{\rm c} = \nu_{\rm syn}(\gamma_{\rm c})$ is the synchrotron cooling frequency above which the synchrotron energy loss becomes important.

The spectral index, p, of shock accelerated electrons is associated with the high-energy power-law photon index, β, of the GRB photon spectrum, by either $\beta = -p/2 - 1$ ('fast cooling' regime) or $\beta = -(p+1)/2$ ('slow cooling' regime) depending on the relative positions of ν_m and $\nu_{\rm c}$ and on which portion of the spectrum is detected. There is one regime, $\nu_{\rm c} < \nu < \nu_m$, in which $\beta = -3/2$, independent of p. This case can be ruled out by discarding those spectra with $\beta \geqslant -3/2$ from our sample. We found only one with $\beta \geqslant -3/2$ in the BATSE sample of 395 spectra and discarded it.

Piran (2004) argues that the fast cooling must take place during the GRB prompt phase and the reasons are: (i) the relativistic shocks must radiate their energy efficiently, to avoid a serious inefficiency problem; (ii) the electrons must cool rapidly in order that the fast variability could be observed. However, there is no firm evidence to date that could rule out the slow cooling case for the GRB itself, since it is difficult to measure the values of $\gamma_{\rm c}$ and $\gamma_{\rm min}$ for a specific burst. Thus in our analysis, we assume that each GRB spectrum above $E_{\rm peak}$ could be in either the slow cooling or fast cooling regime, so as to minimize the width of the p distribution.

First, we plot the distribution of p by assuming all spectra are in the fast cooling regime. Then we make the distribution narrower by relaxing this constraint. Basically, the narrowing process is to move some left-hand part of the distribution to the right by adding 1 to p and assuming this part of the sample are in the slow cooling regime, since there is a difference of 1 about the p value between the two regimes. The algorithm used is described below.

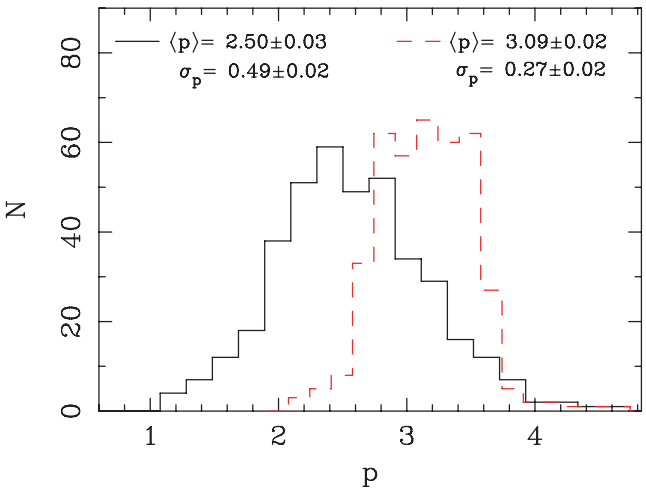

Figure 1. Distributions of p for a sample of 394 GRB spectra with $100 < E_{\rm peak} < 200$ keV. Solid line: using the relation $p = -2\beta - 2$. Dashed line: after narrowing the distribution by using the relation of either $p = -2\beta - 2$ or $p = -2\beta - 1$.

Several algorithms are implemented to get the narrowest distribution. In the most straightforward one, each spectrum has the freedom of calculating p from β either in the 'fast cooling' or in the 'slow cooling' regime, so the number of possible distributions is 2^N for a sample of N spectra. The distribution having the smallest standard deviation is chosen as the narrowest one. This algorithm works well only for $N < 20$ because of the computer running time. For $N > 20$, we divide the overall range of the sample's β distribution into 20 equal-width bins and treat the spectra with β located in each bin indistinguishably. Then we apply the first algorithm to the 20 bins. In an alternative algorithm, we start with the histogram of p calculated in the 'fast cooling' regime and mark a demarcation line within and close to the lower limit of the range of p. Then all p at the left of the line in the histogram are moved to right by adding 1 to p, and the new histogram's standard deviation is calculated. This is repeated after shifting the demarcation line rightward by a step of 0.01 on the p-axis. Finally, the smallest standard deviation, hence the narrowest distribution, is found. It turns out that both algorithms give the same results for most of the samples presented in this paper. For one sample where a minor difference exists between two algorithms' results, we use the narrower one.

We show the results of the analysis for BATSE bursts in Fig. 1. Note that all the errors presented in this paper are at the 1σ level. The parent distribution of p for BATSE bursts has a width of 0.54 at a 14σ confidence level. The method that estimates the mean and the width of the parent distribution of p is described below. Note that the mean value of p is $\approx$3, substantially larger than that for the distribution before the minimization, which is an artefact of choosing some of the spectra to be in the 'slow cooling' regime, equivalent to moving the left part of the histograms in the upper panels rightward, in order to minimize the width of the distribution.

2.3 Statistical description of the narrowness of the *p* distribution

The observed distribution of p plotted in Fig. 1 is a convolution of the measurement error distribution and the true distribution (or parent distribution) of p. What we want to know is the true

distribution of p. We use the maximum likelihood method to estimate the true p distribution. Let us say the true distribution of p is Gaussian,

$$P(p) = \frac{1}{\sqrt{2\pi}\sigma_p} \exp\left[-\frac{1}{2}\frac{(p-\bar{p})^2}{\sigma_p^2}\right]. \quad (3)$$

Further, we assume the measurement errors have Gaussian distributions too. Then the probability distribution for any one measurement (p_i, σ_i) is the convolution of two Gaussians, which is the Gaussian

$$P(p_i, \sigma_i, \bar{p}, \sigma_p) = \frac{1}{\sqrt{2\pi}\left(\sigma_p^2+\sigma_i^2\right)^{1/2}} \exp\left[-\frac{1}{2}\frac{(p_i-\bar{p})^2}{\sigma_p^2+\sigma_i^2}\right]. \quad (4)$$

The likelihood function for the set of n measurements p_i, σ_i is

$$L = \prod_{i=1}^{n} \frac{1}{\sqrt{2\pi}\left(\sigma_p^2+\sigma_i^2\right)^{1/2}} \exp\left[-\frac{1}{2}\frac{(p_i-\bar{p})^2}{\sigma_p^2+\sigma_i^2}\right]. \quad (5)$$

The principle of the maximum likelihood estimate is that the best estimates of $\bar{p}$ and σ_p^2 are the ones that maximize L. Take

$$l = \ln L = -\frac{1}{2}\sum_i^n \frac{(p_i-\bar{p})^2}{\sigma_p^2+\sigma_i^2} - \frac{1}{2}\sum_i^n \ln\left(\sigma_p^2+\sigma_i^2\right), \quad (6)$$

then the maximum occurs when the following equations

$$\left.\frac{\partial l}{\partial \bar{p}}\right|_{\hat{\bar{p}},\hat{\sigma_p^2}} = 0, \quad (7)$$

$$\left.\frac{\partial l}{\partial\left(\sigma_p^2\right)}\right|_{\hat{\bar{p}},\hat{\sigma_p^2}} = 0 \quad (8)$$

have their solution at $\bar{p} = \hat{\bar{p}}$ and $\sigma_p^2 = \hat{\sigma_p^2}$, where '^' symbolizes the best estimation of the parameters. If we assume that the distributions of $\hat{\bar{p}}$ and $\hat{\sigma_p^2}$ are both Gaussian, then one can show that the variances of $\hat{\bar{p}}$ and $\hat{\sigma_p^2}$ are

$$\sigma_{\hat{\bar{p}}}^2 = -\left(\left.\frac{\partial^2 l}{\partial \bar{p}^2}\right|_{\hat{\bar{p}},\hat{\sigma_p^2}}\right)^{-1}, \quad (9)$$

$$\sigma_{\hat{\sigma_p}^2}^2 = -\left[\left.\frac{\partial^2 l}{\partial(\sigma_p^2)^2}\right|_{\hat{\bar{p}},\hat{\sigma_p^2}}\right]^{-1}, \quad (10)$$

respectively. Therefore, the best estimate of the parameters of the true distribution of p is obtained by numerically solving equations (7) and (8), and their associated errors are calculated through equations (9) and (10).

3 SYSTEMATIC ERRORS IN β

3.1 The 'Band' function fit to the spectra

Preece et al. (2000) carried out a Band function fit to GRB spectra observed by BATSE, and this way determined the high-energy power-law index (β) and the random error in β due to error in the observed spectral energy distribution. There is also a systematic error in β resulting from the finite bandwidth of the BATSE detector, which was not reported in Preece et al., and we estimate it here. The purpose of this exercise is to estimate the contribution of this systematic error, and its dependence on the peak of the spectrum ($E_{\rm peak}$), to the dispersion in the p distribution.

The systematic error arises because the synchrotron spectrum does not make a sharp transition from one power-law index to another when one crosses a characteristic frequency. In particular, the steepening of the spectrum to $\nu^{-p/2}$ above the synchrotron and cooling frequencies does not occur suddenly at $E_{\rm peak}$, but instead the spectrum approaches this theoretical value asymptotically at $E \gg E_{\rm peak}$.

Since the spectrum is observed in a finite energy range, the measured spectral index will always be somewhat smaller than the true asymptotic value by an amount that depends on the ratio of $E_{\rm max}$ and $E_{\rm peak}$ ($E_{\rm max}$ is the highest energy photon that the detector is sensitive to). The larger the $E_{\rm max}/E_{\rm peak}$ is the smaller the systematic error in β would be, and this dependence on $E_{\rm peak}$ causes some broadening of the observed β distribution.

To estimate this systematic error, we generate synthetic spectra with different values for $E_{\rm peak}$, and carry out a Band function fit to the synthetic spectra to determine β and its deviation from the true asymptotic value.

The synthetic synchrotron spectra are calculated for a relativistic homogeneous shell. The electron distribution function behind the shock is taken to be a single power-law function $N(\gamma_{\rm e}) \propto \gamma_{\rm e}^{-p}$, for $\gamma > \gamma_{\rm min}$, where $m_{\rm e}c^2\gamma_{\rm min}$ is the minimum electron energy after they cross the shock front. The magnetic field in the shell is taken to be uniform and the energy density of the field is some fraction (ϵ_B) of the thermal energy density of the shocked fluid; $\gamma_{\rm min}$ and ϵ_B are chosen so that the peak of the spectrum, $E_{\rm peak}$, is at some desired value. As electrons move downstream from the shock front, they cool via the synchrotron and inverse-Compton processes, and their distribution function is modified. We calculate the effect of this cooling on electron distribution functions using a self-consistent scheme described in Panaitescu & Mészáros (2000) and McMahon, Kumar & Piran (2006).

The synchrotron spectrum, for a given electron distribution, in the shell comoving frame is calculated as described in detail by Sari, Piran & Narayan (1998) (also see Section 2.2). The spectrum in the observer frame is calculated by integrating the spectral emissivity in the comoving frame over the equal-arrival-time surface as described in Kumar & Panaitescu (2000). Errors are then added to this spectrum in a way that mimics the real GRB spectrum.

The synthetic spectrum for a known p is fitted to the Band function in a finite energy range corresponding to the BATSE energy coverage. By varying $E_{\rm peak}$ of the generated spectra, we determine the discrepancy between the fitted value and 'true' value of β as a function of $E_{\rm max}/E_{\rm peak}$. The results are shown in Fig. 2. We find the fit always gives a smaller β (in absolute value) than the true asymptotic value and that the 'observed' β does indeed depend on $E_{\rm max}$. The error in β is about 10 per cent when $E_{\rm max}/E_{\rm peak}$ is of the order of unity, whereas the error is $\sim$5 per cent when $E_{\rm max}/E_{\rm peak} \sim 20$. The error also depends on the p value as shown in Fig. 2; for $E_{\rm peak}$ located between 100 and 200 keV, $E_{\rm max} = 1.8$ MeV and $p = 2.5$, the contribution of this systematic error to the dispersion in β is less than 1.3 per cent – the corresponding contribution to the dispersion in p is $\sigma_p < 0.03$.

We have also carried out a similar calculation for the SSC spectrum for a population of synchrotron electrons. The incident photons are the synchrotron photons due to the same population of electrons that contribute to inverse-Compton scatterings. The synchrotron radiation is taken to be homogeneous and isotropic in the shell comoving frame, and its spectrum is calculated as described above. The overall SSC spectrum is obtained by the convolution of the synchrotron spectrum and electron energy distribution using equation (7.28a) in Rybicki & Lightman (1979). The curvature in

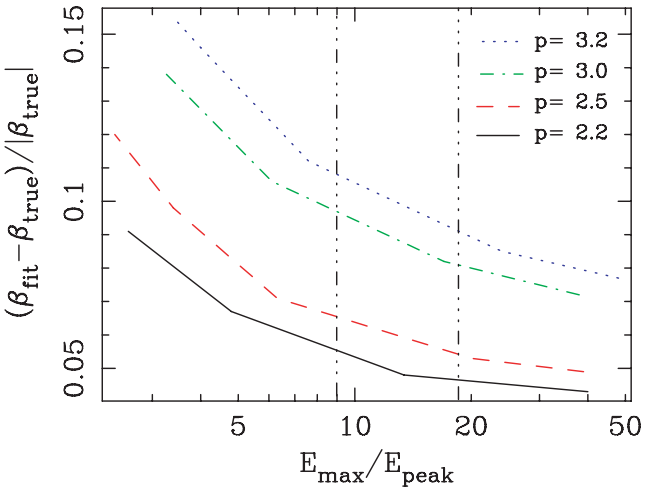

Figure 2. The discrepancy between the fitted value and the 'true' value of β, as a function of the higher end of the fitting energy range for the synchrotron spectra fitted by the 'Band' function. Two vertical lines mark the range of E_{max}/E_{peak} corresponding to the E_{peak} range of the sample in Fig. 1. The errors of the spectrum data are assumed to be proportional to the square root of the photon counts: $\sigma[N(\nu)] \propto \sqrt{N(\nu)}$.

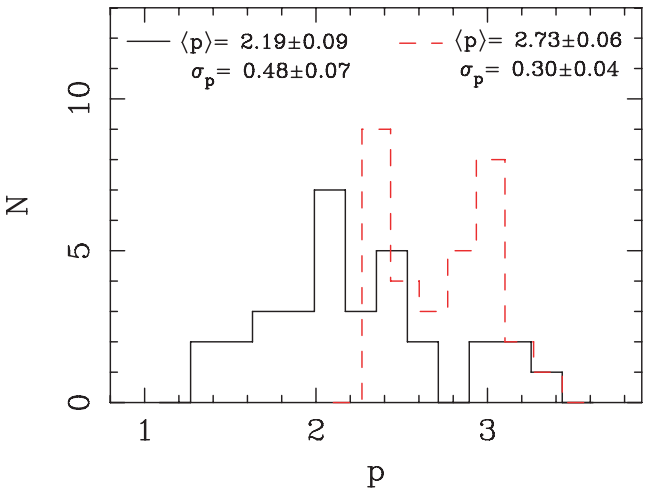

Figure 3. The distribution of p determined from 32 time-integrated GRB spectra. Solid line: p is inferred from the high-energy power-law index β by the relation $p = -2\beta - 2$. Dashed line: the narrowest distribution of p using the relation either $p = -2\beta - 2$ or $p = -2\beta - 1$. β is taken from the 'Band' function fit by Band et al. (1993) to the time-integrated spectrum for each burst.

the SSC spectrum is due to the convolution of the incident spectrum and the electron distribution, and we find that the asymptotic value for the SSC power-law index is reached when $E_{max}/E_{peak} \sim 100$. For this reason, we find that for the SSC case, the systematic error in β is ∼13 per cent for the typical E_{max}/E_{peak} in BATSE bursts. The dispersion in p caused by E_{peak} being distributed between $E_{peak} =$ 100 and 200 keV is, however, small – $\sigma_p < 0.04$.

These results show that the discrepancy between the fitted value and the 'true' value of β is small and dependent on E_{max}/E_{peak}, but its dependence on E_{max}/E_{peak} is too small to account for the observed dispersion in the p distribution.

3.2 Time-averaging effect

Another source of systematic error in β is the time averaging of multiple spectra undergoing spectral evolution, i.e. E_{peak} evolving with flux (Ford et al. 1995; Crider et al. 1999). The flux-weighted time averaging of multiple 'Band' spectra may distort the intrinsic high-energy power law.

To examine this effect, we select BATSE time-resolved spectra with E_{peak} in 100–200 keV and in 200–300 keV, respectively, divide them into non-evolving groups and evolving groups, and analyse their p distributions separately. The results are shown in Table 1. We find the evolving spectra groups tend to have flatter p or β, which may be an outcome of the time-averaging effect. However, the widths of the p distributions for two groups are consistent with each other, showing that the time averaging does not contribute to the observed dispersion in p in Fig. 1.

The time-averaging effect is further examined when we use an early BATSE spectral catalogue by Band et al. (1993) in which the time-integrated spectrum of each burst is fitted with the 'Band' function. We restrict our samples to those with $E_{peak} \leqslant$ 300 keV, and error in β less than $0.1|\beta|$, which gives a sample of 32 spectra from the catalogue of 54 GRBs. The p distribution is shown in Fig. 3. Comparing with Fig. 1, one can see that it has approximately the same σ_p as that for the time-resolved GRB spectra. This supports that the time-averaging effect has no impact on the observed dispersion in p.

4 p DISTRIBUTIONS FOR *BEPPOSAX* GRBs AND *HETE*-2 XRFs, XRR GRBs AND GRBs

We also analysed a sample of 11 GRBs observed by *BeppoSAX*. The combined (2–700 keV) Wide Field Cameras (WFC) and GRB monitor (GRBM) spectra for these bursts are fitted with the 'Band' function by Amati et al. (2002). The narrowest distribution of p for this sample is shown in the left-hand panel of Fig. 4. It has the same estimated mean value of p as in the BATSE bursts, and the width of the parent distribution for p is consistent with that for the BATSE bursts. The larger errors in $\langle p \rangle$ and σ_p are due to the smaller size of the *BeppoSAX* sample.

Sakamoto et al. (2005) present a catalogue of XRFs, XRR GRBs and GRBs observed by the *HETE*-2 Wide Field Camera (WXM) (2–25 keV) and French Gamma Telescope (FREGATE) (7–400 kev) instruments. Among 45 bursts in the catalogue, 16 bursts have measured high-energy power-law photon index, β,

Table 1. Parameters of parent distribution of p for BATSE GRB spectra samples with E_{peak} evolution ($\Delta E_{peak} > 15$ per cent E_{peak}) and without E_{peak} evolution ($\Delta E_{peak} < 15$ per cent E_{peak}), where ΔE_{peak} is the E_{peak} difference between any two *adjacent-in-time* spectra. All spectra are assumed in the 'fast cooling' regime.

	$100 < E_{peak} < 200$ keV		$200 < E_{peak} < 300$ keV	
Spectra samples	Non-evolving	Evolving	Non-evolving	Evolving
$\langle p \rangle$	2.86 ± 0.06	2.38 ± 0.03	2.50 ± 0.07	2.14 ± 0.03
$\sigma(p)$	0.44 ± 0.04	0.47 ± 0.03	0.58 ± 0.06	0.42 ± 0.03

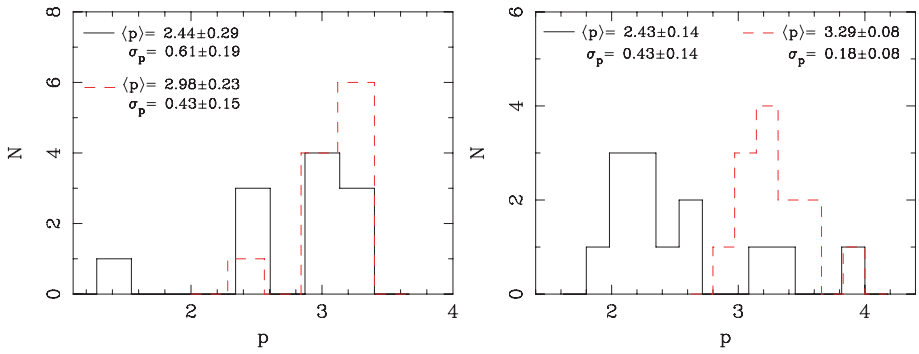

Figure 4. Left-hand panel: the distributions of p for 11 GRBs observed by *BeppoSAX* (Amati et al. 2002); right-hand panel: the distributions of p for 13 XRFs, XRR GRBs and GRBs observed by *HETE*-2 (Sakamoto et al. 2005). Solid lines: p is inferred from the higher energy photon index β by the relation $p = -2\beta - 2$. Dashed lines: the narrowest distributions of p using the relation either $p = -2\beta - 2$ or $p = -2\beta - 1$.

which is obtained through the spectral fit with the 'Band' function or a single power-law model. For those XRF spectra fitted by a single power law, it is found that $\beta < -2$. Sakamoto et al. (2005) explain this as that we are observing the high-energy power-law portion of their 'Band' function spectra. Two GRBs (GRBs 020813 and 030519) for which the 'Band' model is used have $E_{\rm peak}$ lying near or above the upper limit of the FREGATE energy range, so we exclude them here. We also exclude XRF 030528 which has a large error in β. The final *HETE*-2 sample we considered comprises seven XRFs, four XRR GRBs and two GRBs. The p distribution is shown in the right-hand panel of Fig. 4.

5 p DISTRIBUTION FOR X-RAY AFTERGLOWS

We also determine the distribution of p during the X-ray afterglows. We use a catalogue of X-ray afterglows observed by *BeppoSAX* compiled by De Pasquale et al. (2005) and a catalogue of X-ray afterglows observed by *Swift* (O'Brien et al. 2006). In the De Pasquale et al. (2005) catalogue, 15 X-ray afterglow spectra are fitted with a Galactic-and-extragalactic absorbed single power law. We use 14 of them for our analysis and exclude GRB 000210 which has an extremely large error in measured β. In the O'Brien et al. (2006) *Swift* catalogue of 40 X-ray afterglows, we select samples with small errors, $\sigma(\beta_i) < 0.1\,|\beta_i|$, and discard a sample with extremely large $|\beta|$ (=5.5). We also discard four samples with $\beta_i \geqslant -3/2$ because these β values indicate the X-ray band probably lies between $\nu_{\rm c}$ and $\nu_m (\nu_{\rm c} < \nu_{\rm X} < \nu_m)$, where the asymptotic spectral index is $\beta = -3/2$ and carries no information about p. This gives 28 samples from the catalogue.

The p distributions for the two afterglow samples are shown in Fig. 5. For the *BeppoSAX* afterglows, the narrowest distribution is consistent with a δ-function distribution within 1σ errors; for the *Swift* afterglows, it is not. The smaller estimated width of the parent p distribution for *BeppoSAX* afterglows, we suspect, is due to larger errors in photon indices β_i of the *BeppoSAX* sample, $\langle\sigma_i(\beta)\rangle = 0.26$, than the *Swift* sample which has $\langle\sigma_i(\beta)\rangle = 0.10$.

6 DISTRIBUTION OF p IN BLAZARS AND PWNe

6.1 Blazars

Blazars are active galactic nuclei with the relativistic jet pointed towards us. The non-thermal spectra of blazars are due to synchrotron or/and inverse-Compton emission of relativistic electrons accelerated by shocks within the jet (Blandford & Königl 1979; Sikora, Begelman & Rees 1994).

Donato, Sambruna & Gliozzi (2005) present a spectral catalogue of six years of *BeppoSAX* observations of blazars at 0.1–50 keV. This catalogue comprises three classes of blazars, namely low-luminosity sources (high-energy peaked BL Lacs, or HBLs), mid-luminosity sources (low-energy peaked BL Lacs, or LBLs) and high-luminosity sources (flat-spectrum radio quasars, or FSRQs). The three classes have different locations of synchrotron peak. X-rays from

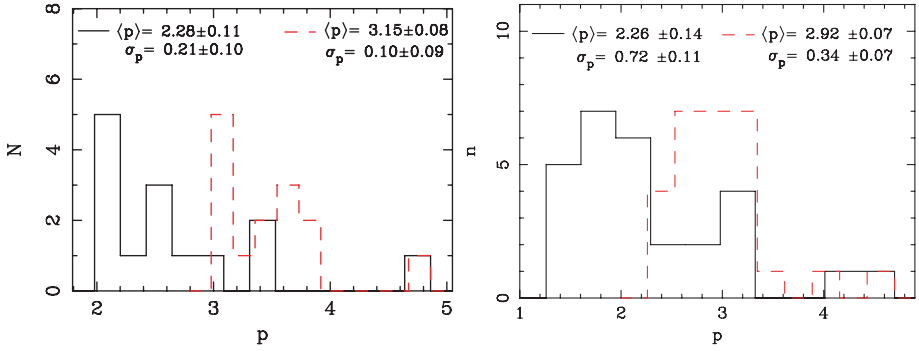

Figure 5. The distributions of p for GRB X-ray afterglows. Left-hand panel: 14 afterglows are observed by *BeppoSAX*, taken from De Pasquale et al. (2005). Right-hand panel: 28 afterglows are observed by *Swift*, taken from O'Brien et al. (2006). Solid lines: p is inferred from the photon index β by the relation $p = -2\beta - 2$. Dashed lines: the narrowest distribution of p using the relation either $p = -2\beta - 2$ or $p = -2\beta - 1$.

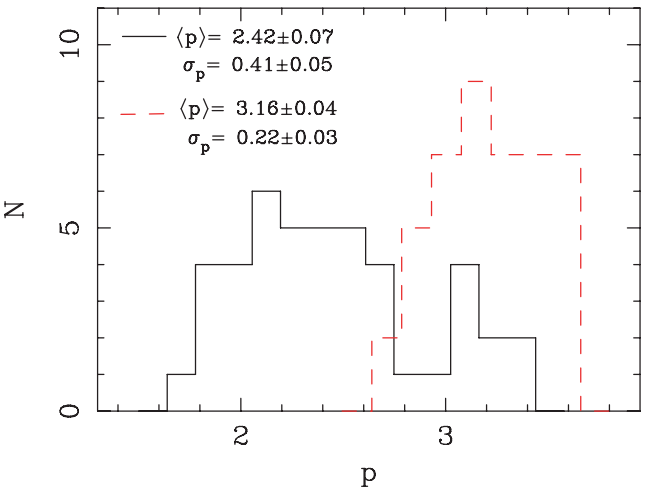

Figure 6. The distribution of p for 44 X-ray spectra of 33 blazars. Solid line: p is inferred from the photon index β by the relation $p = -2\beta - 2$. Dashed line: the narrowest distribution of p using the relation either $p = -2\beta - 2$ or $p = -2\beta - 1$. β is taken from the catalogue compiled by Donato et al. (2005).

HBLs are likely to be above the peak of synchrotron spectrum, thus have steep X-ray spectra ($\beta < -2$), while FSRQs and LBLs in the X-ray band have more contribution from the inverse-Compton component and thus have flatter spectra.

From this catalogue, we use 44 spectra of 33 HBLs (some sources have multi-epoch spectra) that are best fitted by single power laws. The errors of fitted photon indices reported in Donato et al. (2005) are at 90 per cent confidence level which we convert to 1σ errors. The distribution of p derived from their photon spectral indices is shown in Fig. 6. We find that the distribution of p for blazars is not consistent with a δ-function distribution: $\sigma_p = 0.22 \pm 0.03$ after the narrowing.

6.2 Pulsar wind nebulae

Power-law non-thermal spectra are also often observed in PWNe of rotation-powered pulsars. The nebular emission is the synchrotron radiation from charged particles heated by the termination shock in relativistic outflow (winds) from the pulsar (see Arons 2002 for a review). Gotthelf (2003) presents a catalogue of nine bright Crab-like pulsar systems with *Chandra* observations and the photon indices of pulsar nebulae, $\beta_{\rm PWN}$, and their 90 per cent confidence errors are provided. We derive the distribution of p from $\beta_{\rm PWN}$ with the $\beta_{\rm PWN}$ errors converted into 1σ errors and find that $\sigma_p = 0.59 \pm 0.15$, $\langle p \rangle = 1.72 \pm 0.20$ assuming the X-ray band is in the fast-cooling regime. After narrowing, the narrowest distribution has $\sigma_p = 0.24 \pm 0.07$, $\langle p \rangle = 2.04 \pm 0.09$.

7 SUMMARY AND DISCUSSIONS

Motivated by theoretical calculations and numerical simulations showing that the shock-accelerated electrons in relativistic shocks have a power-law distribution with an universal index $p \simeq 2.2$–2.3, we have determined the values of p from gamma-ray and X-ray spectra for a number of relativistic sources such as GRBs (prompt emissions and afterglows), blazars and PWNe.

The maximum likelihood estimate of the width of the parent distribution for GRB prompt emission is found to be quite broad, $\sigma_p = 0.51 \pm 0.02$; the probability that the distribution is consistent with a δ-function is extremely small, and therefore this result does not support that there is a universal p.

We have considered the systematic errors in photon index due to the spectral fit and time averaging of spectra and their contributions to the scatter in the p distribution. We have shown that those contributions are very small for GRBs and cannot explain the scatter in the p distribution.

For X-ray afterglows of GRBs, the p distribution of the *BeppoSAX* sample cannot rule out a possibility that the parent distribution is a δ-function distribution; however, a larger sample of *Swift* afterglows is inconsistent with a δ-function parent distribution. We point out that the smaller width of the parent distribution for the *BeppoSAX* sample is due to its larger measurement error in β.

An analysis of 44 blazars spectra and nine PWNe shows that the distributions of p for blazars and PWNe are also broad, not consistent with a δ-function distribution.

Possible situations in which the 'universality' of p could break are: (i) the shock is mildly relativistic (cf. Kirk et al. 2000); (ii) the magnetic field is oblique to the shock normal (Baring 2005); (iii) the nature and strength of the downstream magnetic turbulence are varying (Ostrowski & Bednarz 2002; Niemiec & Ostrowski 2004). A non-Fermi acceleration in a collisionless plasma shock was studied by Hededal et al. (2004), in which electrons are accelerated and decelerated instantaneously and locally, by the electric and magnetic fields of the current channels formed through the Weibel two-stream instability. It is not known whether a 'universality' of p could hold for this mechanism. The 'universality' of p might not happen in non-shock accelerations; for instance, in an alternative model for GRBs (Lyutikov & Blandford 2003), the energy is carried outwards via magnetic field or Poynting flux. The particles accounting for the gamma-ray emissions are accelerated by magnetic field reconnection which may also produce a power-law spectrum of accelerated particles with a variable p (however, this is still poorly understood).

ACKNOWLEDGMENTS

This work was supported in part by a NSF (AST-0406878) grant and a NASA-Swift-GI grant. RS thanks Dr Volker Bromm for his suggestion which helps to improve this work.

REFERENCES

Achterberg A., Gallant Y. A., Kirk J. C., Guthemann A. W., 2001, MNRAS, 328, 393
Amati A. et al., 2002, A&A, 390, 81
Arons J., 2002, in Slane P. O., Gaensler B. M., eds, ASP Conf. Ser. Vol. 271, Neutron Stars in Supernova Remnants. Astron Soc. Pac., San Francisco, p. 71
Band D. et al., 1993, ApJ, 413, 281
Baring M. G., 2005, Adv. Space Res., in press (astro-ph/0502156)
Bednarz J., Ostrowski M., 1998, Phys. Rev. Lett., 80, 3911
Blandford R. D., Königl A., 1979, ApJ, 232, 34
Blandford R. D., Ostriker J. P., 1978, ApJ, 221, L29
Crider A. et al., 1999, ApJ, 519, 206
De Pasquale M. et al., 2005, A&A, in press (astro-ph/0507708)
Donato D., Sambruna R. M., Gliozzi M., 2005, A&A, 433, 1163
Ford L. A. et al., 1995, ApJ, 439, 307
Gotthelf E. V., 2003, ApJ, 591, 361
Hededal C. B., Haugbølle T., Frederiksen J. T., Nordlund Å., 2004, ApJ, 617, L107
Kirk J. G., Guthmann A. W., Gallant Y. A., Achterberg A., 2000, ApJ, 542, 235

Kumar P., Panaitescu A., 2000, ApJ, 541, L9
Lemoine M., Pelletier G., 2003, ApJ, 589, L73
Lyutikov M., Blandford R., 2003, preprint (astro-ph/0312347)
McMahon E., Kumar P., Piran T., 2006, MNRAS, 366, 575
Niemiec J., Ostrowski M., 2004, ApJ, 610, 851
O'Brien P. T. et al., 2006, ApJ, in press (astro-ph/0601125)
Ostrowski M., Bednarz J., 2002, A&A, 394, 1141
Panaitescu A., Mészáros P., 2000, ApJ, 544, L17
Piran T., 2004, Rev. Mod. Phys., 76, 1143
Preece R. D., Pendleton G. N., Briggs M. S., Mallozzi R. S., Paciesas W. S., Band D. L., Matteson J. L., 1998, ApJ, 496, 849
Preece R. D., Briggs M. S., Mallozzi R. S., Pendleton G. N., Paciesas W. S., Band D. L., 2000, ApJS, 126, 19
Preece R. D., Briggs M. S., Giblin T. W., Mallozzi R. S., Pendleton G. N., Paciesas W. S., Band D. L., 2002, ApJ, 581, 1248
Rybicki B. G., Lightman A. P., 1979, Radiative Processes in Astrophysics. John Wiley & Sons Inc.
Sakamoto T. et al., 2005, ApJ, 629, 311
Sari R., Piran T., Narayan R., 1998, ApJ, 497, L17
Sikora M., Begelman M. C., Rees M. J., 1994, ApJ, 421, 153

This paper has been typeset from a TEX/LATEX file prepared by the author.